Available online at www.sciencedirect.com

ScienceDirect

Carbohydrate Polymers 70 (2007) 166–173

Carbohydrate Polymers

www.elsevier.com/locate/carbpol

Synthesis and characterization of chitosan-g-poly(acrylic acid)/sodium humate superabsorbent

Jianghua Liu [a,b], Qin Wang [a,b], Aiqin Wang [a,*]

[a] Center of Eco-Material and Green Chemistry, Lanzhou Institute of Chemical Physics, Chinese Academy of Sciences, Lanzhou 730000, PR China
[b] Graduate University of the Chinese Academy of Sciences, Beijing 100049, PR China

Received 6 February 2007; received in revised form 7 March 2007; accepted 23 March 2007
Available online 30 March 2007

Abstract

A novel chitosan-g-poly(acrylic acid)/sodium humate (CTS-g-PAA/SH) multifunctional superabsorbent was prepared by graft polymerization among chitosan, acrylic acid and sodium humate in aqueous solution, using *N*,*N*′-methylenebisacrylamide as a crosslinker and ammonium persulfate as an initiator. And the samples were further characterized by means of FTIR, SEM and TGA. The effect of polymerization variables, including reaction temperature, content of initiator, crosslinker and sodium humate, the weight ratio of acrylic acid to chitosan, on water absorbency were studied. The swelling rate in distilled water and the swelling behavior in various pH value solutions were also investigated. The result from FTIR spectra showed that chitosan and sodium humate participated in graft polymerization reaction with acrylic acid. The introduced sodium humate could enhance water absorbency and the content of 10 wt% sodium humate gave the best absorption (183 g g^{-1} in distilled water and 41 g g^{-1} in 0.9 wt% NaCl solution).

Keywords: Chitosan; Sodium humate; Superabsorbent; Water absorbency; Swelling behavior

---

1. Introduction

Superabsorbents are loosely crosslinked network of hydrophilic polymers that can absorb and retain a lot of aqueous fluids, and the absorbed water is hardly removable even under some pressure. Compared with traditional absorbing materials, superabsorbents have many excellent properties and are widely used in many fields, such as hygienic products, horticulture, gel actuators, drug-delivery systems and coal dewatering (Buchholz & Graham, 1998; Shiga, Hirose, Okada, & Kurauchi, 1992; Dorkoosh et al., 2000; Raju, Raju, & Mohan, 2003; Ende, Hariharan, & Peppas, 1995). However, most of the superabsorbents are acrylic acid and acrylamide based products and cannot be biodegraded in nature. Thus, the superabsorbents and hydrogels with eco-friendly property and biodegradability are finding increasing interest in the academic and industrial field (Lionetto, Sannino, & Maffezzoli, 2005).

Superabsorbents prepared with natural material, such as cellulose (Farag & Al-Afaleq, 2002), starch (Kiatkamjornwong, Mongkolsawat, & Sonsuk, 2002; Li, Zhang, & Wang, 2007) and chitosan (Ge, Pang, & Luo, 2006), because of their abundant resources, low production-cost and biodegradability, have attracted great attention. Chitosan, a high molecular weight polysaccharide from chitin, is the second most abundant natural polymers after cellulose. Chitosan is excellent biodegradable biomass and can be degraded into nontoxic products in vivo. It has both reactive $–NH_2$ and –OH that can be convenient for graft polymerization of hydrophilic vinyl monomers onto it under mild reaction condition, and the acquired superabsorbent resin can absorb aqueous solution hundreds of times than their own dry sample (Nge, Hori, Takemura, & Ono, 2004) and should have antibacterial activities (No, Park, Lee, Hwang, & Meyers, 2002). So, this type superabsorbents can be used in many special fields (No et al., 2002; Dutkiewicz, 2002).

---

[*] Corresponding author. Tel.: +86 931 4968118; fax: +86 931 8277088.
E-mail address: aqwang@lzb.ac.cn (A. Wang).

0144-8617/$ - see front matter © 2007 Published by Elsevier Ltd.
doi:10.1016/j.carbpol.2007.03.015

Widening the properties of superabsorbents is of interesting work. Superabsorbents with slow release fertilizer properties have also received much attention, because it is as important as water in the arid and desert environment. Sodium humate from turf is composed of multifunctional aliphatic components and aromatic constituents, and contains a large number of functional groups (such as carboxylates and phenolic hydroxyls) (Hayes, MacCarthy, Malcolm, & Swift, 1989). Sodium humate can regulate plant growth, accelerate root development, enhance photosynthesis, improve soil cluster structures and benefit the absorption of nutrient elements. It has been reported in our previous work on the poly (acrylic acid-co-acrylamide)/sodium humate (Zhang, Li, & Wang, 2006) and poly (acrylic acid-co-acrylamide)/sodium humate/attapulgite (Zhang, Li, & Wang, 2005) that sodium humate had good slow release fertilizer properties and could enhance plant growth very well in the soil.

In order to obtain multifunctional superabsorbent with biodegradable and slow release fertilizer properties, on the basis of our previous work on superabsorbent composites (Zhang, Wang, & Wang, 2007; Zhang et al., 2006), a novel chitosan-g-poly(acrylic acid)/sodium humate (CTS-g-PAA/SH) superabsorbent was synthesized, and swelling behaviors of the superabsorbent were also investigated in this paper.

2. Experimental

2.1. Materials

Acrylic acid (AA, chemically pure, distilled under reduced pressure before use), ammonium persulfate (APS, analytical grade, recrystallized from distilled water before use) and *N*,*N*′-methylenebisacrylamide (MBA, chemically pure used as received) were supplied by Shanghai Reagent Corp. (Shanghai, China). Chitosan (CTS, degree of deacetylation is 0.90, average molecular weight is 20×10^4) was supplied by Zhejiang Yuhuan Ocean Biology Co. (Zhejiang, China). Sodium humate (SH, milled though a 320-mesh screen before use) was supplied by Shuanglong Ltd, (Xinjiang, China). Other agents used were all of analytical grade and all solutions were prepared with distilled water.

2.2. Preparation of chitosan-g-poly(acrylic acid)/sodium humate (CTS-g-PAA/SH) superabsorbent

A series of superabsorbent from CTS, AA and SH were synthesized according to the following procedure. Appropriate amount of CTS was dissolved in 30 ml acetic acid solution (1%) in a 250 ml four-neck flask, equipped with a mechanical stirrer, a reflux condenser, a funnel and a nitrogen line. After being purged with nitrogen for 30 min to remove the oxygen dissolved from the system, and certain amount of APS was introduced to initiate CTS to generate radicals. Ten minutes later, the mixed solution of 3.60 g AA, certain amount of MBA and SH, and 10 ml water was added. The water bath was kept at 80 °C for 3 h to complete the polymerization. The resulting product was transferred into sodium hydroxide aqueous solution (2 M) to be neutralized to pH 7, and then the samples were spread on a dish to dry to a constant weight at 70 °C in an oven. The product was milled and all samples used for test had a particle size in the range of 40–80 mesh. The feed compositions of all samples were listed in Table 1.

CTS-g-PAA (without SH) was prepared according to the same procedure to study the effect of introduced SH on properties of the superabsorbent.

2.3. Measurement of water absorbency

Sample of 0.05 g was immersed in excess distilled water (50 ml) at room temperature for 4 h to reach swelling equilibrium. Swollen samples were then separated from unabsorbed water by filtering through a 100-mesh screen under gravity for 10 min and no blotting of samples. Water absorbency in distilled water of the superabsorbent, Q_{eq}, was calculated using the following equation:

$$Q_{eq} = \frac{m_2 - m_1}{m_1} \tag{1}$$

where m_1 and m_2 are the weights of the dry sample and the swollen sample, respectively. Q_{eq} is calculated as grams of water per gram of sample. Water absorbency of the sample in 0.9 wt% NaCl solution, Q'_{eq}, was tested according to the same procedure.

Table 1
Feed compositions of CTS-g-PAA/SH superabsorbent

Samples code	AA(g)	CTS(g)	APS(g)	MBA(g)	SH(g)
APS1	3.60	0.50	0.050	0.150	0.50
APS2	3.60	0.50	0.075	0.150	0.50
APS3	3.60	0.50	0.100	0.150	0.50
APS4	3.60	0.50	0.125	0.150	0.50
APS5	3.60	0.50	0.150	0.150	0.50
APS6	3.60	0.50	0.175	0.150	0.50
APS7	3.60	0.50	0.200	0.150	0.50
MBA1	3.60	0.50	0.150	0.075	0.50
MBA2	3.60	0.50	0.150	0.100	0.50
MBA3	3.60	0.50	0.150	0.125	0.50
MBA4	3.60	0.50	0.150	0.150	0.50
MBA5	3.60	0.50	0.150	0.175	0.50
MBA6	3.60	0.50	0.150	0.200	0.50
CTS1	3.60	0.40	0.150	0.150	0.50
CTS2	3.60	0.50	0.150	0.150	0.50
CTS3	3.60	0.60	0.150	0.150	0.50
CTS4	3.60	0.72	0.150	0.150	0.50
CTS5	3.60	0.90	0.150	0.150	0.50
SH1	3.60	0.50	0.150	0.150	0.00
SH2	3.60	0.50	0.150	0.150	0.23
SH3	3.60	0.50	0.150	0.150	0.50
SH4	3.60	0.50	0.150	0.150	1.10
SH5	3.60	0.50	0.150	0.150	1.89
SH6	3.60	0.50	0.150	0.150	2.93

2.4. Measurement of water absorbency in various pH value solutions and swelling rate in distilled water

The pH of external solutions was adjusted using 1 M NaOH or HCl aqueous solutions. The method used was the same as the water absorbency in distilled water. Swelling rate of superabsorbent was measured according to the previous reported method (Omidian, Hashemi, Sammes, & Meldrum, 1998).

2.5. Characterization

IR spectra of samples were taken as KBr pellets using a Thermo Nicolet NEXUS TM spectrophotometer. The micrographs of samples were taken using SEM (JSM-5600LV, JEOL, Ltd.). Before SEM observation, all samples were fixed on aluminum stubs and coated with gold. Thermal stability of samples was studied on a Perkin–Elmer TGA-7 thermogravimetric analyzer (Perkin–Elmer Cetus Instruments, Norwalk, CT), with a temperature range of 25–800 °C at a heating rate of 10 °C min^{-1} using dry nitrogen purge at a flow rate of 50 ml min^{-1}.

3. Results and discussion

3.1. IR spectra

The FTIR spectra of SH, CTS-g-PAA, CTS-g-PAA/SH superabsorbent incorporated with 10 and 30 wt% SH are shown in Fig. 1. Comparing with the spectrum of SH (Fig. 1(a)), the absorption band at 3216 and 3071 cm^{-1} (N–H stretching) and 2358 cm^{-1} (O–H stretching of carboxylic group) are absent in the spectra of CTS-g-PAA/SH superabsorbent (Fig. 1(c) and (d)). Comparing with the spectrum of CTS-g-PAA (Fig. 1(b)), the adsorption band at 1558 cm^{-1} (COO^- asymmetric stretching) as well as 1068 cm^{-1} (C–O stretching) shifts to 1562 cm^{-1}, 1106 cm^{-1} in the spectra of CTS-g-PAA/SH superabsorbent containing 10 wt% SH (Fig. 1(c)). In addition, the new adsorption band at 1703 cm^{-1}, which is attributed to C=O stretching of carboxylic group of SH, appears in the spectra of CTS-g-PAA/SH superabsorbent containing 10 wt% and 30 wt% (Fig. 1(c) and (d)). It can be concluded from the FTIR information that some chemical reactions occurred during the polymerization process. However, the adsorption band of CTS-g-PAA/SH superabsorbent containing 30 wt% SH at 1562 cm^{-1} almost disappears and the new adsorption band at 1632 cm^{-1} appears (Fig. 1(d)), which indicates that the introduced more SH may have some influence on chemical environment of the hydrophilic $–\text{COO}^-$ group, and excess SH may be only act as filler in the CTS-g-PAA/SH polymeric network.

3.2. Thermal stability

The thermogravimetric analysis (TGA) of CTS-g-PAA and CTS-g-PAA/SH superabsorbent are shown in Fig. 2. As can be seen from Fig. 2, as the temperature increased from room temperature to 377 °C, the weight loss of

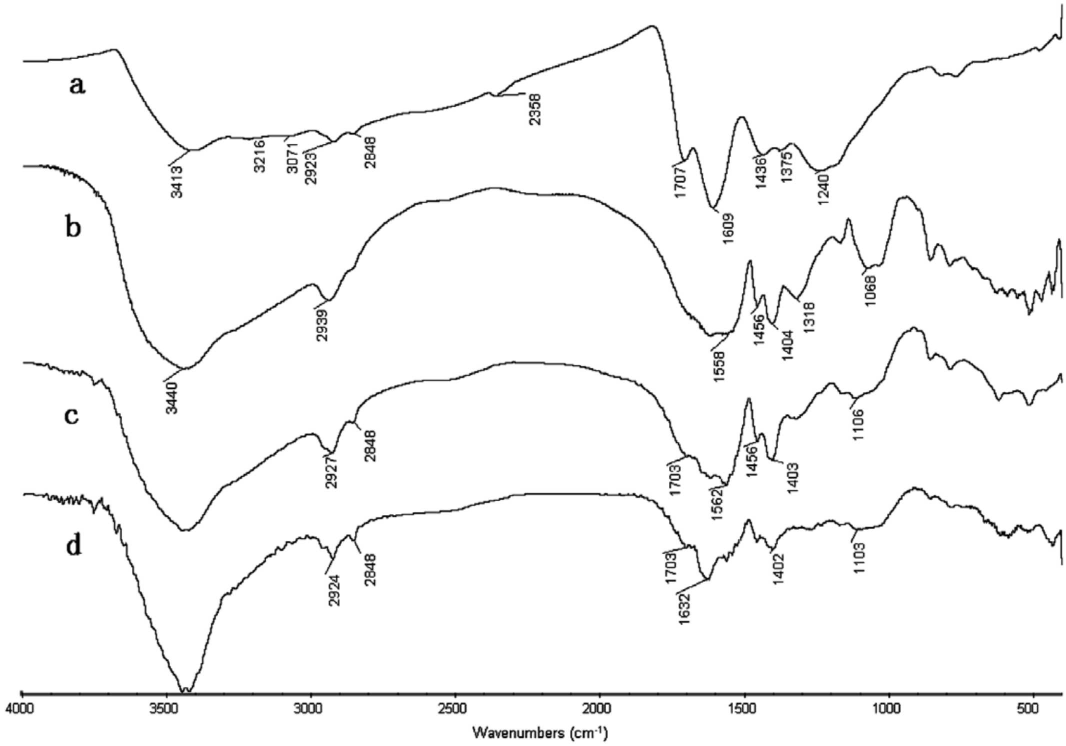

Fig. 1. FTIR spectra of SH (a), CTS-g-PAA (b) and CTS-g-PAA/SH superabsorbent incorporated with 10 wt% SH (c) and 30 wt% SH (d).

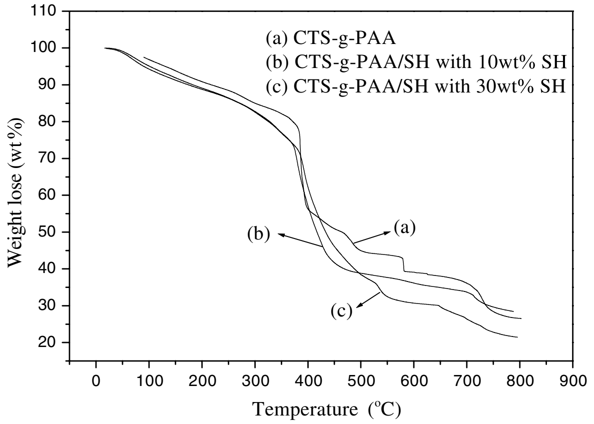

Fig. 2. TGA curves of CTS-g-PAA (a) and CTS-g-PAA/SH superabsorbent (b and c).

CTS-g-PAA and CTA-g-PAA/SH superabsorbent are associated with a complex progress, including the evaporation of water present in the samples, dehydraten of saccharide rings and breaking of C–O–C glycosidic bonds in the main chain of CTS (Douglas & Sergio, 2004). There was prominent difference between CTS-g-PAA and CTS-g-PAA/SH superabsorbent in the temperature range of 377–531 °C. For CTS-g-PAA, it exhibits a two-stage thermal decomposition process in this temperature range. The first thermal decomposition process with 21% weight loss corresponds to decomposition of the carboxyl groups of PAA chain, and the second step with 9% weight loss is attributed to the breakage of the chains of PAA. Similar thermal behavior has been reported by Chen et al. for carboxymethylchitosan-g-poly(acrylic acid) (Chen & Tan, 2006). Comparing with CTS-g-PAA, CTS-g-PAA/SH superabsorbent showed larger total weight loss within this temperature range, and the more SH content, the higher total weight loss, implying not only the decomposition of PAA chain, but also the decomposition of SH. As may be observed in the TGA curves (Fig. 2), CTS-g-PAA/SH superabsorbent showed higher total weight loss as a whole comparing with CTS-g-PAA. This result indicated that the introduction of SH into CTS-g-PAA polymeric network results in a decrease in thermal stability.

3.3. Morphological analysis

The SEM micrographs of the internal structure of CTS-g-PAA and CTS-g-PAA/SH superabsorbent incorporated with 30 wt% SH are shown in Fig. 3. As can be seen, CTS-g-PAA shows a porous and rough surface. However, the introduction of SH results in CTS-g-PAA/SH superabsorbent forming a fewer porous and tight surface. It can be concluded from Fig. 3 that SH has great influence on surface morphology of the superabsorbent. This surface morphology change by introducing SH indicates the interaction among CTS, PAA and SH, and then may has some influence on swelling ability of corresponding superabsorbent.

3.4. Effect of reaction temperature on water absorbency

The effect of reaction temperature on water absorbency for superabsorbent is investigated and shown in Fig. 4. As can be seen, water absorbency increases in distilled water and in 0.9 wt% NaCl solution with increasing reaction temperature from 50 to 90 °C. When the reaction temperature is increased, the rate of polymerization also increases, which results in the decrease of crosslingking efficiency

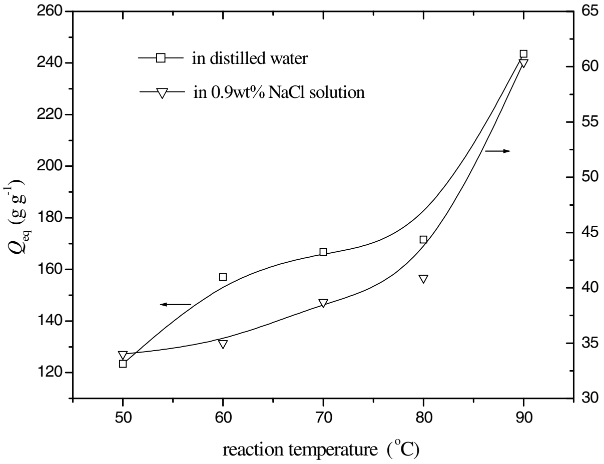

Fig. 4. Variation of Q_{H_2O} in distilled water and 0.9 wt% NaCl solution with reaction temperature for CTS-g-PAA/SH. The weight ratio of CTS, SH, initiator and crosslinker to acrylic acid is 13.9, 13.9, 2.78 and 4.17 wt%, respectively.

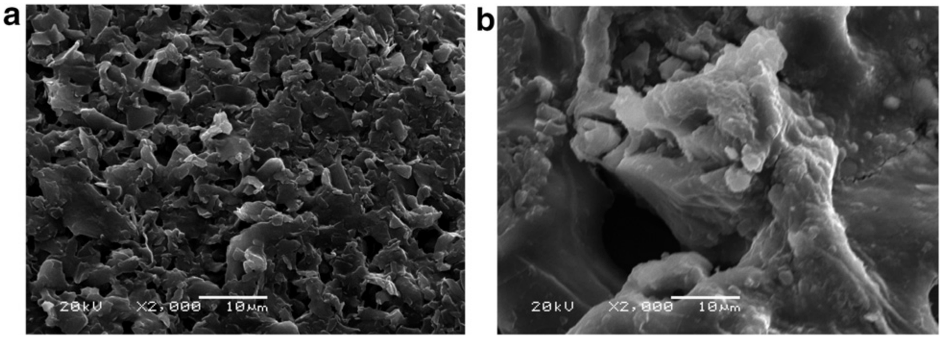

Fig. 3. SEM micrographs of CTS-g-PAA (a) and CTS-g-PAA/SH superabsorbent incorporated with 30 wt% SH (b).

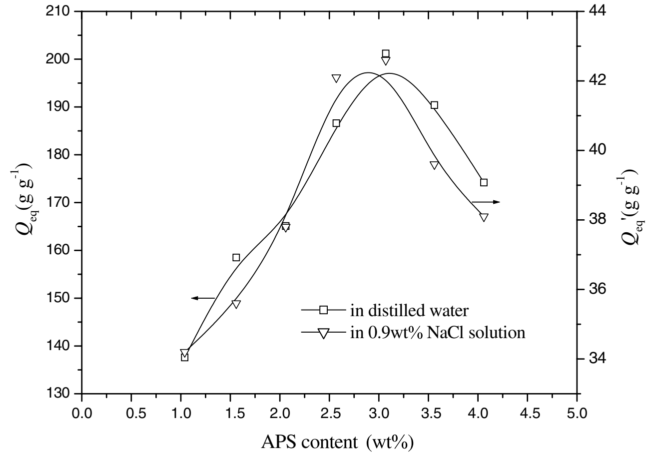

Fig. 5. Variation of $Q_{\mathrm{H_2O}}$ in distilled water and 0.9 wt% NaCl solution with initiator content for CTS-g-PAA/SH. Reaction temperature, 80 °C. The weight ratio of CTS, SH and crosslinker to acrylic acid is 13.9, 13.9 and 4.17 wt%, respectively.

(Chen & Zhao, 1999). At the same crosslinker content, the water absorbency increases with the decrease of crosslinking efficiency according to Flory's network theory (Flory, 1953). It has been reported previously by us on the poly(acrylic acid)/attapulgite polymeric network that the absorbency increases from 40 °C to 70 °C but decreases with further increase in the reaction temperature (Li, Wang, & Chen, 2004), However, the water absorbency for CTS-g-PAA/SH superabsorbent increases continuously with increase of reaction temperature, This result indicates that introducing SH and clay into the poly(acrylic acid) network have different interaction mechanism. Due to the product was not uniformity at 90 °C, 80 °C was recommended for further study.

3.5. Effect of initiator content on water absorbency

The effect of initiator content on water absorbency for superabsorbent is shown in Fig. 5. As can be seen, the water absorbency increases with increasing APS content from 1.0 to 3.0 wt% and then decreases with further increase in the content of APS. According to the relation between the average kinetic chain length and concentration of initiator in free-radical polymerization, the molecular weight grafted on polymer backbone will decrease with increase of initiator concentration and then more polymer chain ends generated. As mentioned in previous study (Liu & Rempel, 1997), the polymer chain ends do not contribute to water absorbency of superabsorbent. So, further increasing initiator content from 3.0 to 4.0 wt% is responsible for the decrease of water absorbency. However, the water absorbency decreases with decreasing initiator content below optimum value. This is attributed to the fact that the network cannot form efficiently and simultaneously more water-soluble materials owing to the fact the deficient radicals were generated as the content of initiator decreased.

3.6. Effect of crosslinker content on water absorbency

The effect of crosslinker content on water absorbency is shown in Fig. 6. It is obvious that water absorbency decreases with increase of crosslinker content in the range of 2.5–4.0 wt%. As crosslinker content increases, more crosslink points generate during the polymerization, which causes the formation of an additional network, and decreases the space left for water to enter. This is in conformity with Flory's network theory (Flory, 1953). When the crosslinker content is lower than 2.5 wt%, the water absorbency of superabsorbent is diminished because of an increase of soluble materials.

3.7. Effect of weight ratio of AA to CTS on water absorbency

The effect of weight ratio of AA to CTS on water absorbency of the CTS-g-AA/SH superabsorbent is investigated and shown in Fig. 7. It can be seen from Fig. 7 that the

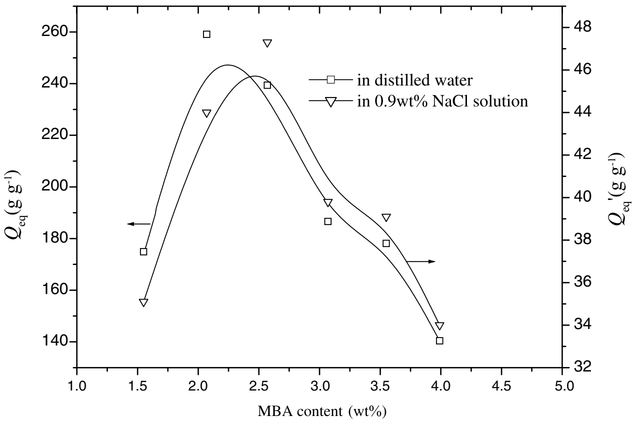

Fig. 6. Variation of $Q_{\mathrm{H_2O}}$ in distilled water and 0.9 wt% NaCl solution with crosslinker content for CTS-g-PAA/SH. Reaction temperature, 80 °C. The weight ratio of CTS, SH and initiator to acrylic acid is 13.9, 13.9 and 4.17 wt%, respectively.

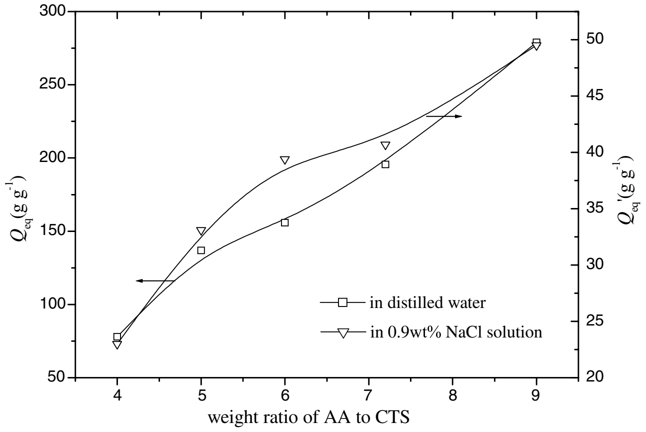

Fig. 7. Variation of $Q_{\mathrm{H_2O}}$ in distilled water and 0.9 wt % NaCl solution with weight ratio of AA to CTS for CTS-g-PAA/SH. Reaction temperature, 80 °C. The weight ratio of SH, initiator and crosslinker to acrylic acid is 13.9, 4.17 and 4.17 wt%, respectively.

water absorbency increases continuously with increasing weight ratio of AA to CTS in the range of experimental tested. The increasing water absorbency with increasing weight ratio of AA to CTS can be explained as follows. As the weight ratio of AA to CTS increases, the higher monomer concentration would cause more AA molecules to be grafted onto the backbone of CTS, which enhanced hydrophilicy of corresponding superabsorbent and consequently caused an increase in water absorbency. In addition, more mobile Na^+ ions generated in the polymeric network owing to the neutralization of PAA chains of the superabsorbent. Consequently, osmotic pressure difference between polymeric network and external solution increased. Moreover, molecular weight of grafted PAA chains increased which also contributed to the improvement of water absorbency.

3.8. Effect of SH content on water absorbency

The effect of SH content on water absorbency for the CTS-g-AA/SH superabsorbent is shown in Fig. 8. As can be seen, the water absorbency increases with increasing amount of SH in the weight range of 0–10%. Water absorbency for the superabsorbent is enhanced from 135 to 183 g g^{-1} by introducing 10 wt% SH into the CTS-g-AA polymeric network. And even when 40 wt% SH is introduced, the water absorbency for the multifunctional superabsorbent in distilled water is still higher than that of pure CTS-g-AA, which significantly reduces production cost of the superabsorbent.

SH, complex organic macromolecules, contains free and bound phenolic –OH groups, quinine structure, nitrogen and oxygen as bridge units, –COOH and $–NH_2$ groups variously placed on aromatic ring (Paciolla, Kalla, & Jansen, 2002; Dicicco, duong, Chu, & Jansen, 2003). Those functional groups of SH can react with CTS and AA during polymerization progress. At the same crosslinker content, the introduction of SH into CTS-g-PAA polymeric network could decrease the effective crosslinking density, which result in the increasing water absorbency with increasing SH content in the weight range of 0–10%. However, when the SH content is above 10 wt%, the decrease of water absorbency is attributed to the fact that the excess SH only acts as filler, which result in decrease of the effect space to hold more water. It has been reported by Wu, Wei, Lin, and Lin (2003) on the starch-graft-acrylamide/mineral powder system that excess kaolin particles are physically filled in the network. So, the decrease of water absorbency for the CTS-g-AA/SH polymeric network may be attributed to a similar mechanism.

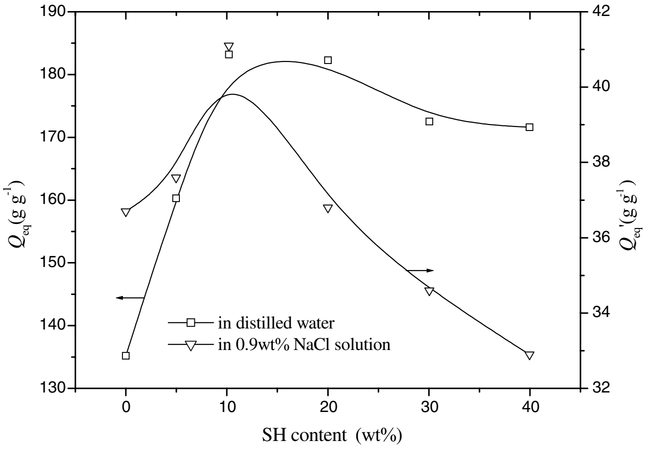

Fig. 8. Variation of Q_{H_2O} in distilled water and 0.9 wt% NaCl solution with SH content for CTS-g-PAA/SH. Reaction temperature, 80 °C; the weight ratio of CTS, initiator, crosslinker to acrylic acid is 13.9, 8.3 and 8.3 wt%, respectively.

3.9. Effect of SH content on water absorbency in various pH value solutions

The swelling behavior of CTS-g-PAA and CTS-g-PAA/SH superabsorbent in various pH value solutions is investigated and shown in Fig. 9. It can be seen that the water absorbency for the CTS-g-PAA/SH superaborbent is always higher than that of CTS-g-PAA, and the water absorbency for CTS-g-PAA/SH superaborbent incorporated with 10 wt% SH is almost higher than that of CTS-g-PAA/SH superaborbent incorporated with 30 wt% SH. The water absorbency for CTS-g-PAA and CTS-g-PAA/SH superabsorbents roughly maintains a constant from pH 4 to 11. This swelling behavior can be explained by the buffer action of –COOH and $–COO^-$ with acid or base, as previously reported by Lee and Wu (1996, 1997). Because in weak acidic or basic environment, the –COOH groups and $–COO^-$ groups on the polymeric chains can partially transform one another. In addition, the water absorbency increases sharply from pH 2 to 4 and drastically decreases from pH 11 to 13, which indicates that the buffer action has vanished. This is because the pH value in external solutions is too low or too high. When the pH value is to high, most of $–COO^-$ groups change into

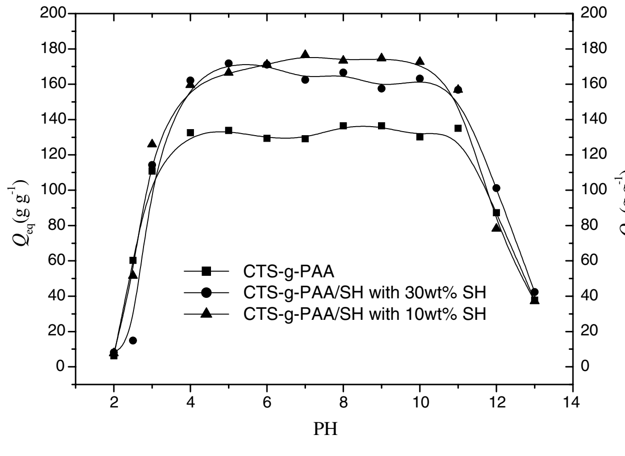

Fig. 9. Effect of pH on water absorbency of CTS-g-PAA and CTS-g-PAA/SH superaborbent.

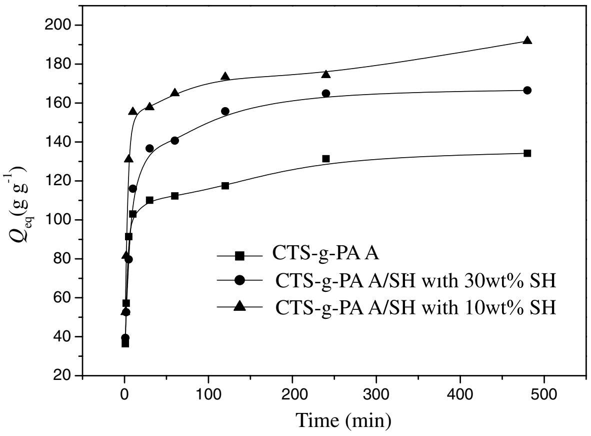

Fig. 10. Swelling rate in distilled water for CTS-g-PAA and CTS-g-PAA/SH superabsorbent.

–COOH groups, which results in the decrease of repulsion among polymeric chains and consequentially leads to decrease of water absorbency; When the pH value is to low, most of –COOH groups change into $-COO^-$ groups, which results in the increase of the screening effect of the counterion on the polyanion chains and also leads to decrease of water absorbency.

3.10. Effect of SH content on swelling rate

According to Buchanan, Hird, and Letcher (1986) report, the swelling rate of a superabsorbent is significantly influenced by swelling capacity, size distribution of powder particles, specific surface area, and apparent density of polymer. Fig. 10 shows the swelling rate for CTS-g-PAA and CTS-g-PAA/SH superabsorbent in distilled water. As can be seen, the curves for CTS-g-PAA/SH superabsorbent are flatter than that for CTS-g-PAA. In addition, CTS-g-PAA/SH superabsorbent prepared with 30 wt% of SH exhibited lower swelling rate and required more time to reach absorption equilibrium comparing with CTS-g-PAA/SH superabsorbent incorporated with 10 wt% SH. According to Lee and Wu (1996) report, the initial swelling progress is due primarily to the water penetrating into polymeric network through capillarity and diffusion. The percentage of hydrophilic groups (such as –COOH and –COO–) on polymeric network for CTS-g-PAA/SH superabsorbent decreased with increasing SH content. So the diffusion rate of water penetrating into inside of superabsorbent decreased. Therefore, the superabsorbent with more SH showed lower initial swelling rate and needed more time to reach equilibrium water absorbency.

4. Conclusions

A novel CTS-g-PAA/SH superabsorbent with biodegradable and eco-friendly properties was prepared by grafted copolymerization reaction through CTS and AA in the presence of SH in aqueous solution. Various factors including reaction temperature, amount of initiator, crosslinker and SH, the weigh ratio of AA to CTS have great influence on water absorbency of the CTS-g-PAA/APT superabsorbent. Introducing SH could improve water absorbency of the CTS-g-PAA superabsorbent. CTS-g-PAA/SH superabsorbent not only can reduce significantly production cost, but also promotes new functional properties.

Acknowledgements

This work was financially supported with the Western Action Project of CAS (No. KGCX2-YW-501) and "863" Project of the Ministry of Science and Technology, PR China (No. 2006AA03Z0454).

References

Buchholz, F. L., & Graham, T. (1998). *Modern superabsorbent polymer technology*. NewYork: Wiley-VCH.

Buchanan, K. J., Hird, B., & Letcher, T. M. (1986). Crosslinked poly(sodium acrylate) hydrogels. *Polymer Bulletin, 15*, 325–332.

Chen, J. W., & Zhao, Y. M. (1999). An efficient preparation method for superabsorbent polymers. *Journal of applied polymer science, 74*, 119–124.

Chen, Y., & Tan, H. M. (2006). Crosslinked carboxymethylchitosan-g-poly(acrylic acid) copolymer as a novel superabsorbent polymer. *Carbohydrate Research, 341*, 887–896.

Dicicco, M., duong, T., Chu, A., & Jansen, S. A. (2003). Tobramycin and Gentamycin elution analysis between two in situ polymerizable orthopedic composites. *Journal of Biomedical Material Research, 65*, 137–149.

Dorkoosh, F. A., Brussee, J., Verhoef, J. C., Borchard, G., Tehrani, M. R., & Junginger, H. E. (2000). Preparation and NMR characterization of superporous hydrogels (SPH) and SPH composites. *Polymer, 41*, 8213–8220.

Douglas, D. B., & Sergio, P. C. F. (2004). A kinetic study on the thermal degradation of *N,N,N*-trimethylchitosan. *Polymer Degradation Stability, 84*, 353–361.

Dutkiewicz, J. K. (2002). Superabsorbent materials from shellfish waste – A review. *Journal Biomedical Materials Research, 63*, 373–381.

Ende, M., Hariharan, D., & Peppas, N. A. (1995). Factors influencing drug and protein transport and release from ionic hydrogels. *Reactive Polymers, 25*, 127–137.

Farag, S., & Al-Afaleq, E. I. (2002). Preparation and characterization of saponified delignified cellulose polyacrylonitrile-graft copolymer. *Carbohydrate Polymers, 48*, 1–5.

Flory, P. J. (1953). *Principles of polymer chemistry*. Ithaca, NY: Cornell University Press.

Ge, H. C., Pang, W., & Luo, D. K. (2006). Graft copolymerization of chitosan with acrylic acid under microwave irradiation and its water absorbency. *Carbohydrate Polymers, 66*, 372–378.

Hayes, M. H. B., MacCarthy, P., Malcolm, R. L., Swift, R. S. (Eds.) (1989). *Humic substances II: In search of structure.* New York: Wiley.

Kiatkamjornwong, S., Mongkolsawat, K., & Sonsuk, M. (2002). Synthesis and property characterization of cassava starch grafted poly[acrylamide-co-(maleic acid)] superabsorbent via γ-irradiation. *Polymer, 43*, 3915–3924.

Lee, W. F., & Wu, R. J. (1996). Superabsorbent polymeric materials. I. Swelling behaviors of crosslinked poly(sodium acrylate-co-hydroxyethyl methacrylate) in aqueous salt solution. *Journal of Applied Polymer Science, 62*, 1099–1114.

Lee, W. F., & Wu, R. J. (1997). Superabsorbent polymeric materials. IV. Swelling behavior of crosslinked poly[sodium acrylate-co-*N,N*-

dimethyl (acrylamidopropyl) ammonium propane sulfonate] in aqueous salt solution. *Journal of Applied Polymer Science, 66*, 499–507.

Li, A., Zhang, J. P., & Wang, A. Q. (2007). Utilization of starch and clay for preparation of superabsorbent. *Bioresource Technology, 98*, 327–332.

Li, A., Wang, A. Q., & Chen, J. M. (2004). Study on poly(acrylic acid)/attapulgite superabsorbent. I. Synthesis and characterization. *Journal of Applied Polymer Science, 92*, 1596–1603.

Lionetto, F., Sannino, A., & Maffezzoli, A. (2005). Ultrasonic monitoring of the network formation in superabsorbent cellulose based hydrogels. *Polymer, 46*, 1796–1803.

Liu, Z. S., & Rempel, G. L. (1997). Preparation of superabsorbent polymers by crosslinking acrylic acid and acrylamide copolymers. *Journal of Applied Polymer Science, 64*, 1345–1353.

Nge, T. T., Hori, N., Takemura, A., & Ono, H. (2004). Swelling behavior of chitosan/poly(acrylic acid) complex. *Journal of Applied Polymer Science, 92*, 2930–2940.

No, H. K., Park, N. Y., Lee, S. H., Hwang, H. J., & Meyers, S. P. (2002). Antibacterial activity of chitosans and chitosan oligomers with different molecular weights. *Journal of Food Science, 67*, 1511–1514.

Omidian, H., Hashemi, S. A., Sammes, P. G., & Meldrum, I. G. (1998). Modified acrylic-based superabsorbent polymers. Effect of temperature and initiator concentration. *Polymer, 39*, 3459–3466.

Paciolla, M. D., Kalla, S., & Jansen, S. A. (2002). The reduction of dissolved iron species by humic acid and subsequent production of reactive oxygen species. *Advances in Environmental Research, 7*, 169–178.

Raju, K. M., Raju, M. P., & Mohan, Y. M. (2003). Synthesis of superabsorbent copolymers as water manageable materials. *Polymer International, 52*, 768–772.

Shiga, T., Hirose, Y., Okada, A., & Kurauchi, T. (1992). Bending of poly(vinyl alcohol)-poly(sodium acrylate) hydrogel in electric fields. *Journal of Applied Polymer Science, 44*, 249–253.

Wu, J. H., Wei, Y. L., Lin, J. M., & Lin, S. B. (2003). Study on starch-graft-acrylamide/mineral powder superabsorbent composite. *Polymer, 44*, 6513–6520.

Zhang, J. P., Li, A., & Wang, A. Q. (2006). Synthesis and characterization of multifunctional poly(acrylic acid-co-acrylamide)/sodium humate superabsorbent composite. *Reactive and Functional Polymers, 66*, 747–756.

Zhang, J. P., Li, A., & Wang, A. Q. (2005). Study on superabsorbent composite. V. synthesis, swelling behaviors and application of poly(acrylic acid-co-acrylamide)/sodium humate/attapulgite superabsorbent. *Polymer for Advanced Technology, 16*, 813–820.

Zhang, J. P., Wang, Q., & Wang, A. Q. (2007). Synthesis and characterization of chitosan-g-poly(acrylic acid)/attapulgite superabsorbent composites. *Carbohydrate Polymers, 68*, 367–374.